Detection of burned forests in Amazonia using the Normalized Burn Ratio (NBR) and Linear Spectral Mixture Model from Landsat 8 images

Laura Barbosa Vedovato[1]
Aline Daniele Jacon [1]
Ana Carolina Moreira Pessôa [1]
André Lima [1]
Luiz Eduardo Oliveira e Cruz de Aragão[1]

[1] Instituto Nacional de Pesquisas Espaciais - INPE
Caixa Postal 515 - 12227-010 - São José dos Campos - SP, Brasil
{aline, ana, laurabv}@dsr.inpe.br

Abstract. Wildfires represent a major disturbance factor leading to environmental changes with local or regional impacts. In the Amazon, although fire is associated with several land-practices, the long dry season in some regions, especially during extreme droughts, makes vegetation more susceptible to uncontrolled fires. Furthermore, the burn of biomass is a considerable source of atmospheric pollution, including carbon dioxide, a major greenhouse gas. Due to the large geographical extent of fires at regional and global scales, remote sensing approaches became relevant in the last decades.. In this paper, we compare two different methodologies of fire detection for Amazon region and evaluate possible spectral confusions these two methods can generate on the analysis. We compared the Normalized Burn Ratio (NBR) and the Linear Spectral Mixture Model data extracted from high resolution satellite Landsat 8 image. Our results indicate that the detection of burned forests areas using the LSMM index performs better over fragmented landscapes, with a index Kappa of 0.68 and 0.66 against a index Kappa for NBR of 0.52 and 0.52, in the study sites B and C respectively. Considering areas less fragmented as study site A in this study, both methodologies showed the same Kappa value (0.88). Thus, considering the complexity of Amazonian landscapes, which encompass both high and low fragmentation areas, the LSMM index is likely to perform better in the detection of burnt forests than the NBR index. .

Key Words: remote sensing, image processing, Normalized Burn Ratio, Linear Spectral Mixture Model, fire, Amazon.

1. Introduction

Fire represents a major disturbance factor. It is considered an agent of environmental change with local and regional impacts regarding land use, productivity, biodiversity, hydrology, biogeochemistry, and atmospheric processes (Csiszar et al. 2004). According to Crutzen and Andreae (1990), biomass burning is one of the most important sources of atmospheric pollution due to the release of trace gases and aerosols. The understory wildfires emit substantial carbon to the atmosphere and are a catalyst of forest degradation and potential substitution by savanna, invasive grassland, or scrub species (Balch et al. 2011). Fire is also considered an important ecosystem process affecting vegetation structure and composition (Johnson and Miyanishi, 1997) and it can indicate land cover change in many land use systems (Cochrane, 2003). Over the past few decades, human-ignited, understory wildfires have become more frequent and intense in several tropical regions (Balch et al. 2011).

Amazon wildfires are thought to be almost exclusively human ignited due to the high density of ignition sources associated with fire-dependent land practices (Anderson et al. 2005). Although Cardoso et al. (2008) pointed out to a high density of lightning flashes in this region. The Amazon experiences two distinctive seasons during the year, a dry and a wet one. The majority of fire detections occur during the dry season (Aragão et al. 2007). During this period, higher water deficits, temperatures and higher fuel availability, increase the susceptibly of Amazonian vegetation to accidental fires. (Anderson *et al.,* 2005; Laurance and Williamson, 2001).

One of the critical variables necessary to quantify the magnitude of wildfire impact is the size of the affected area. Considering Amazonia's extensive area and access constraints, the use of remote sensing approaches become relevant. Remote sensing technologies can provide

useful data for fire management, from risk estimation, fire detection, fuel mapping, to post fire monitoring, including burn area and severity estimation (Lanorte et al. 2013). Even though within the field of remote sensing of fire, the detection of burned areas is relatively well established (Roy et al. 2005), not all problems were solved yet. There are spectral confusions between burned surfaces and water bodies, urban areas, shades and between slightly burned land and unburned vegetation that is associated mainly with mixed pixels (Chuvieco and Congalton, 1988; Koutsias et al. 1999). Different regions with variable conditions, such as topography, deforestation status, or near to water bodies can have the detection of fires made by distinctive methodologies.

The aim of this paper is to compare two different methodologies of fire detection for Amazon region and evaluate possible spectral confusions that these two methods can generate on the analysis. We compared the Normalized Burn Ratio (NBR) and the Linear Spectral Mixture Model (LSMM) outputs extracted from high resolution satellite Landsat 8 image.

2. Study area

The study area was located in the northern portion of the Brazilian state of Mato Grosso, Central-West Brazil. This was defined by a Landsat scene within the path 227 and row 67 from July, 26th, 2014 (Figure 1).
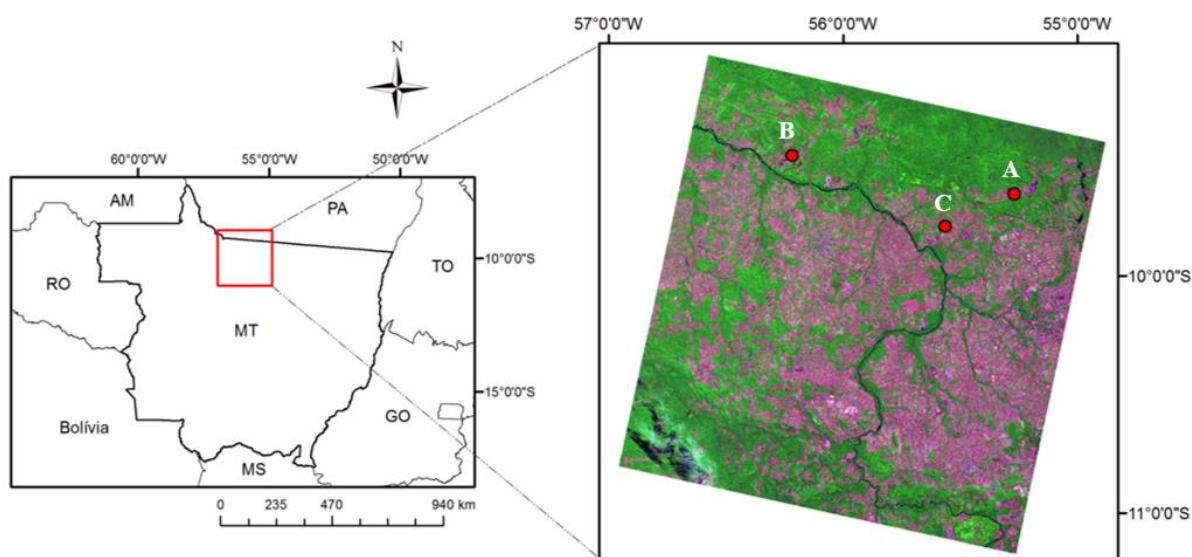

Figure 1. Study area location. A, B and C corresponds to the areas analyzed within the scene OLI Landsat 8 (path/row 227/67; Datum WGS84; R6G5B4).

In the northern flank of the state of Mato Grosso, the average annual temperature is about 26°C and the average annual rainfall can be higher than 2.700 mm (Nimer, 1977 apud Anderson et al. 2005). However, precipitation is not equally distributed throughout the year. More than 70% of total rainfall is concentrated in the rainy season that happens between November and March. The drier months are distributed between May and October (Anderson et al. 2005). Burning is one of the processes contributing to the high rates of land cover conversion (INPE, 2005).

We chose three study areas within the scene based on the presence of burned forest areas and the presence of targets that could possibly generate spectral confusion in the two methods applied. The targets considered were water body, bare soil (including croplands and deforestation areas), and rocky outcrop. The locations A and C are within the city of Novo Mundo, and the location B within the city of Alta Floresta. The coordinates of the locations are:

Location A (55°16'3.362"W and 9°39'25.08"S), Location B (56°12'56.144"W and 9°29'53.073"S), and Location C (55°33'45.365"W and 9°47'38.247"S). The locations A and C were chosen due to the presence of bare soil nearby burned areas. The location B also presents bare soil nearby burned area, in addition to rocky outcrops and water bodies.

3. Data and Methodology

3.1 Image Acquisition

The OLI scene used on this study was downloaded from USGS website (USGS, 2014) and it corresponded to the Julian day 207 (July 26th) of 2014. The date was chosen because of the high number of hotspots (57 hotspots) registered by INPE (INPE, 2012) and lack of clouds. We used six of its 11 spectral bands ((band 2 (0.452-0.512μm), band 3(0.533-0.590 μm), band 4 (0.636-0.673 μm), band 5 (0.851-0.879 μm), band 6 (1.566-1.651 μm) and band 7(2,107-2.294 μm)), going from visible region until short-wave infrared region of the electromagnetic spectrum, all with 30 m spatial resolution. We then created a single six bands stacked layer for subsequent processing using ENVI version 5.0.

3.2 Atmospheric correction

The OLI scene was atmospherically corrected through the application of the FLAASH algorithm, available in ENVI. This technique uses the radiative transfer model, called MODTRAN, to perform the correction. This pre-processing step was carried out to minimize the scattering effects of the atmosphere on the spectral characterization of targets. Prior to the atmospheric correction, we converted the image values from digital numbers to radiance and subsequently to surface reflectance.

All other image processing was carried out using SPRING, version 5.2.

3.3 Data sets

A deforestation mask for the same path/row was downloaded from PRODES program and overlapped to the original Landsat image (INPE, 2005). The mask was downloaded for 2013, since it was the most updated data that matches our image from 2014. None of the deforestation-delimited polygons coincided within our study areas. This fact reinforced that our definition of area of burned forests was independent from recent deforestation. Active fire data detected two months before the image acquisition were also downloaded and overlapped to the image (INPE, 2012). The active fire data was used to guide the delimitation of burned areas. With the assistance of these ancillary data and the help of a specialist, the burned areas were delimited in the three study locations (Figure 1).

3.4 Linear Spectral Mixture Model (LSMM)

The LSM Model utilizes a linear relationship to represent the proportional spectral contribution of different targets to the reflectance of a single pixel. The algorithm requires the selection of endmembers for each target considered in the analysis. These endmembers must represent the pure spectral signature of the respective target. We considered three endmembers for the analysis: (1) vegetation - selected on homogeneou crop plantation, avoiding the presence of shades and bare soil, (2) soil - selected on bare soil areas, and (3) shade - selected on black water bodie without sediments. The selection of the endmembers was made directly from the image, through selection of pixels with spectral signature as close as possible of the theoretical curve of pure pixels. The LSMM can be defined according to the following equation (Equation 1):

$$r_i = a*vegetation_i + b*soil_i + c*shade_i + e_i \qquad (Eq.\ 1)$$

Where r_i is the reflectance of the pixel related to band i; a, b and c are the proportional fractions of vegetation, soil and shade, respectively, to be estimated by the model; $vegetation_i$,$soil_i$ and $shade_i$ are the spectral signatures of the three endmembers: vegetation, soil and shade, respectively; e_i indicates the error. We derived the fraction images based on the six bands stacked image. The shade image was used for subsequent comparison with the NBR index, as this fraction is widely used to map fire scars (ANDERSON et al. 2005).

3.5 NBR Index

The Normalized Burn Ratio (NBR) was formulated as an index to detect burned areas. It is presented as a reliable means to map fire severity, computed as the difference between near infrared (NIR) and middle-infrared (MIR) reflectance divided by their sum. These bands are used because they present the best contrast between photosynthetic healthy vegetation and burned vegetation. Besides that, an increase of band MIR reflectance, due to decreased water absorption by the canopy, followed by a decrease on NIR can be seen on burned areas (LANORTE et al. 2013).

The NBR can be defined by the following equation (Equation 2), considering the OLI bands:

$$NBR = (R_5 - R_7) / (R_5 + R_7) \hspace{4cm} \text{(Eq. 2)}$$

Where R_5 and R_7 correspond to the reflectance of bands 5 and 7 of the OLI sensor.

The NBR was calculated using arithmetic operations implemented in the software SPRING, which requires values for gain and offset in order to improve the contrast in the final image. It was used a gain of 100 and 0 for offset. The NBR image presents burned areas as dark regions (low NBR values).

3.6 Analysis

The comparison between the two methodologies to detect burned forest areas was made qualitatively through evaluation of the performance of the segmentation algorithm, compared with the reference area of burned forests and quantitatively using the confusion matrix and the index Kappa.

For the qualitative evaluation of the two models we first segmented the output images using a region growth algorithm with similarity and area (pixels) values of 8 and 25, respectively. Segmentation algorithms aim to partitioning homogeneous and continuous areas based on the degree of similarity of pixels established by the user. The segments created represent regions built by pixels with similar reflectance, obeying the similarity rule imposed (8 of similarity, and 25 pixels of area).

4. Results and Discussion

Figure 2 shows the three sites analyzed with delimited areas that represent the fire scars and the hotspots registered from June to July pointed by red circles.
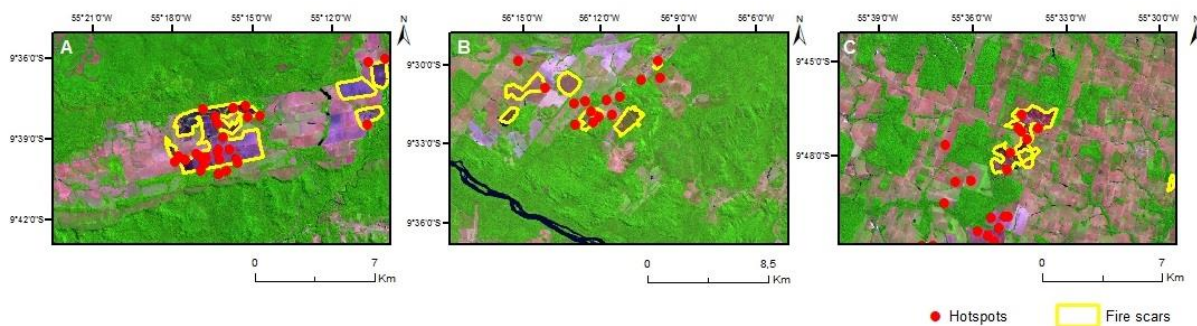
Figure 2. Sites of study with fire scars in yellow and hotspots in red circles.

Figure 3 presents the results of the segmented shade image, generated by LSMM (Figure 3A, B and C), and the results of the segmented NBR image (Figure 3D, E and F).
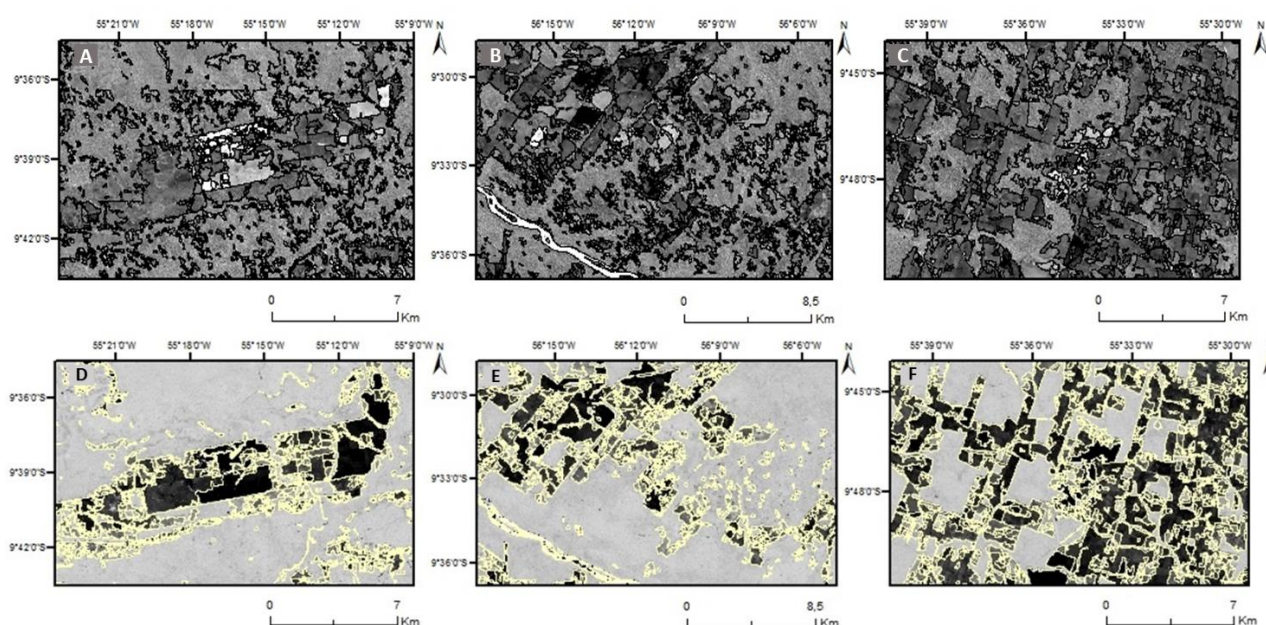

Figure 3. The letters A, B and C are results of the segmented image LSMM for sites A, B and C, respectively, and the letters D, E and F are results of segmented image NBR for the same sites as in the top panel.

The brighter areas in the shade fraction image (Figure 3A, B and C) indicate a greater proportion of the shade component in pixels. This feature is found on targets of low reflectance in all spectral bands (Shimabukuro and Smith, 1991). As an example of these targets, burned areas, water bodies, shade of clouds and topography can be mentioned (Chuvieco, 1996). Therefore, polygons representing burned areas should be brighter in the image, facilitating their discrimination against other targets.

When compared to the original image, the shade fraction highlights fire scars in larger dimension areas (Figure 3A). In fragmented areas (Figure 3B and C), the pattern of segmented burned forests is not as clear in the shade fraction image due to the small size and shape variations of the areas in the landscape. The spectral confusion, as expected for water, occurs in the segmented image.

Moreover, a large spectral confusion was observed between bare soil and burned areas, indicating that such areas, initially identified as areas of recent fires, can actually represent different stages of post-fire. With the gradual decline of ash inside burned areas, and the onset of vegetation regrowth, reflectance values become composed by the mixture of substrate and regrowth. The low reflectance values along the whole electromagnetic spectrum, typically

registered in recent burned areas, changes gradually as the vegetation starts to grow (Person and Meneses, 2013). So, a critical next step is to answer why burned areas, depending on their stage of recovery, can behave similarly to the bare soil, including croplands.

Opposing to the shade fraction image, generated by LSMM, NBR image relates the low reflectance of dark hue pixels. Targets like as previously seen, burned areas, water bodies, rocky outcrops, cloud shade among others, register low reflectance values and, hence, are represented by dark hue pixels in the NBR image.

When comparing the original image of the first study site (Figure 2A) with the synthetic NBR one (Figure 3D), it can be observed that the index responded consistently distinguishing the burned areas in most cases. There is only a small degree of confusion with areas of bare soil.

For the study sites B and C (Figure 2B and C) the potential of index NBR on detecting fire scars decreased (Figure 3E and F), due to the greater amount of bare soil present in this areas. This confusion could be explained by the similarity of the spectral response of these targets that was previously mentioned. The areas of rocky outcrop were also not confused with burned areas.

Table 1 shows the values of commission and omission errors, overall accuracy and de index Kappa for LSMM and NBR index for each area analyzed.

Table 1. Results of confusion matrix and index Kappa

	A		B		C	
	LSMM	NBR	LSMM	NBR	LSMM	NBR
Commission (%)	12	12	32	48	34	48
Omission (%)	11.7	11.3	30.9	43.4	25.4	44.8
Overall Accuracy (%)	94	94	84	76	83	76
Index Kappa	0.88	0.88	0.68	0.52	0.66	0.52

In site A both indices, LSMM and NBR performed similarly, with an index Kappa of 88%. In sites B and C, the LSMM index had higher overall accuracy (84% and 83% for sites B and C respectively) and Kappa values (68% and 66% for sites B and C respectively) than the NBR index (Table 1). With the results we can observed that for less fragmented sites both index can be used to separate burned forest areas from other targets. However, for more fragmented sites LSMM index achieves a better result.

In general, the NBR index did not behave in a consistent manner in order to distinguish burned areas. The reason of this behavior can be attributed to spectral confusion found between bare soil and water bodies and the interest areas. The non-efficiency of the index can also be attributed to the sizes of the burned fragments. Small fragments may hide the border separation of the targets.

5. Final Considerations

The detection of burned forests using the LSMM index proved to have similar performance on recognizing large burned areas when compared to the NBR index. Considering fragmented areas, i.e. small dimension of burned areas, the LSMM index overcomes the performance of the NBR index, despite a reduction of the overall accuracy in relation to areas less fragmented. Thus, considering the complexity of Amazonian landscapes, which encompass both high and low fragmentation areas, the LSMM index is likely to perform better in the detection of burnt forests than the NBR index.

A possible alternative to improve the detection of fire scars is temporal image analysis (Morton et al. 2011), considering pre-fire and post-fire data. It allows the estimation of differences image, what facilitates the identification and enhances the accuracy of burned areas detection methodologies.

Acknowledgements

References

Anderson, L. O.; Aragão, L. E. C. De; Lima, A. De. Detecção de cicatrizes de áreas queimadas baseada no modelo linear de mistura espectral e imagens índice de vegetação utilizando dados multitemporais do sensor MODIS/TERRA no estado do Mato Grosso, Amazônia brasileira. **Acta Amazonica**, v. 35, n. 4, p. 445–456, 2005.

Aragão, L. E. O. C.; Malhi, Y.; Roman-cuesta, R. M.; Saatchi, S.; Anderson, L. O.; Shimabukuro, Y. E. Spatial patterns and fire response of recent Amazonian droughts. **Geophysical Research Letters**, v. 34, n. 7, p. L07701, 3 abr. 2007.

Balch, J. K.; Nepstad, D. C.; Curran, L. M.; Brando, P. M.; Portela, O.; Guilherme, P.; Reuning-scherer, J. D.; De Carvalho, O. Size, species, and fire behavior predict tree and liana mortality from experimental burns in the Brazilian Amazon. **Forest Ecology and Management**, v. 261, n. 1, p. 68–77, jan. 2011.

Cardoso, M. F.; Nobre, C. A.; Lapola, D. M.; Oyama, M. D.; Sampaio, G. Long-term potential for fires in estimates of the occurrence of savannas in the tropics. **Global Ecology and Biogeography**, v. 17, n. 2, p. 222–235, mar. 2008.

Chuvieco, E.; Congalton, R. G. Mapping and inventory of forest fires from digital processing of tm data. **Geocarto International**, v. 3, n. 4, p. 41–53, dez. 1988.

Chuvieco, E. **Fundamentos de teledetección espacial**. Madrid: Ediciones Rialp.1996. 568p

Cochrane, M. A. Fire science for rainforests. **Nature**, v. 421, n. 6926, p. 913–9, 27 fev. 2003.

Crutzen, P. J.; Andreae, M. O. Biomass burning in the tropics: impact on atmospheric chemistry and biogeochemical cycles. **Science (New York, N.Y.)**, v. 250, n. 4988, p. 1669–78, 21 dez. 1990.

Csiszar, I.; Justice, C. O.; Mcguire, A. D.; Cochrane, M. A.; Roy, D. P.; Brown, F., ET AL. In: Gutman, G.; Janetos, A. C.; Justice, C. O.; Moran, E. F.; Mustard, J. F.; Rindfuss, R. R.; Skole, D.; Turner II, B. L.; Cochrane, M. A. (Org.). **Land use and fires. Land change science: Observing, monitoring, and understanding trajectories of change on the earth's surface**. [S.l.]: Kluwer Academic Publishers, 2004.

Instituto Nacional de Pesquisas Espaciais (INPE). **Monitoramento da floresta Amazônica brasileira por satellite**. [S.l: s.n.] , 2005. Disponível em: <www.obt.inpe.br/prodes/seminario2005>.

Instituto Nacional De Pesquisas Espaciais (INPE). **Portal de monitoramento de queimadas e incêncios**. 2012. Disponível em: <www.inpe.br/queimadas>. Acesso em: 9 dez. 2014.

Johnson, E. A.; Miyanishi, K. **Forest Fires: Behavior and Ecological Effects**. San Diego, CA: Academic Press, 1997.

Koutsias, N.; Karteris, M.; Fernandez-Palacios, A.; Navarro, C.; Jurado, J.; Navarro, R.; Lobo, R. In: Chuvieco, E. (Org.). **Burned land mapping at local scale**. Berlin: Springer-Verlag, 1999. 157–187 p.

Lanorte, A.; Danese, M.; Lasaponara, R.; Murgante, B. Multiscale mapping of burn area and severity using multisensor satellite data and spatial autocorrelation analysis. **International Journal of Applied Earth Observation and Geoinformation**, v. 20, p. 42–51, fev. 2013.

Laurance, W. F.; Williamson, G. B. Positive feedbacks among forest fragmentation , drought, and climate change in the Amazon. **Conservation Biology**, v. 15, n. 6, p. 1529–1535, 2001.

Morton, Douglas C.; DeFries, Ruth S.; Nagol, Jyoteshwar; Souza Jr., Carlos M.; Kasischke, Eric S.; Hurtt, George C.; Dubayah, Ralph. 2011. Mapping canopy damage from understory fires in Amazon forests using annual time series of Landsat and MODIS data. Remote Sensing of Environment 115(7):1706-1720.

Pessoa, O. A. A.; Meneses, P. R. Evolução do comportamento espectral de cicatrizes de incêndio florestal no Cerrado. In: SIMPÓSIO BRASILEIRO DE SENSORIAMENTO REMOTO, 16. (SBSR), 2013, Foz do Iguaçu. **Anais...** São José dos Campos: INPE, 2013. p. 3314-3320.

Roy, D. P.; Jin, Y.; Lewis, P. E.; Justice, C. O. Prototyping a global algorithm for systematic fire-affected area mapping using MODIS time series data. **Remote Sensing of Environment**, v. 97, n. 2, p. 137–162, jul. 2005.
Shimabukuro, Y.E., Smith, J.A. The Least-Squares Mixing Models to Generate Fraction Images Derived From Remote Sensing Multispectral Data. **IEEE Transactions on Geoscience and Remote Sensing**, Vol. 29, p. 16-20, 1991.

United States Geological Survey Earth Explorer (USGS). Available in: <http://earthexplorer.usgs.gov/> Acess: 10/09/2014.